Computational Mathematics and Mathematical Physics, Vol. 45, No. 3, 2005, pp. 444–453.
Translated from Zhurnal Vychislitel'noi Matematiki i Matematicheskoi Fiziki, Vol. 45, No. 3, 2005, pp. 462–471.

Solution of Singularly Perturbed Convection–Diffusion Problems by the Local Green's Function Method

E. V. Glushkov, N. V. Glushkova, and D. V. Timofeev

Kuban State University, Krasnodar, 350080 Russia
e-mail: evg@math.kubsu.ru, nvg@math.kubsu.ru

Received January 29, 2004

Abstract—As applied to one-dimensional singularly perturbed problems, methods based on local Green's functions exhibit fast convergence and numerical stability even if the problems involve sharp boundary layers. However, such methods virtually were not applied to problems in two or more space variables, since local Green's functions cannot be derived in a closed analytical form in these cases. In the present paper two-dimensional convection–diffusion problems are used as an example to show high efficiency of the Petrov–Galerkin discretization scheme in which the load Green's functions are used as projectors. The Green's functions are constructed on the basis of semianalytical integral representations proposed earlier. Asymptotic expansions of the Green's functions are also derived. They remove the existing limits of the practical applicability of the method with respect to the singularity parameter ε tending to zero. Test comparisons and numerical examples for an inhomogeneous convection field demonstrate numerical stability of the solutions with minimal costs, which stabilize as $\varepsilon \longrightarrow 0$.

Keywords: singularly perturbed convection–diffusion problems, solution based on the local Green's function method.

1. INTRODUCTION

The convection–diffusion equation

$$\mathcal{L}u \equiv -\varepsilon\Delta u + \mathbf{b}\cdot\nabla u + cu = f, \quad \mathbf{x} \in \Omega \subset \mathbb{R}^d, \tag{1.1}$$

describes the steady transport of particles by a convective velocity field $\mathbf{b}(\mathbf{x})$ in the presence of weak diffusion ($\varepsilon/|\mathbf{b}| \ll 1$) and is a classical example of equations with a small parameter multiplying the highest derivatives. Boundary value problems for such equations are known to be singularly perturbed and their solutions can involve boundary and interior layers with steep gradients (on the order of $O(1/\varepsilon)$) [1, 2].

For example, in the Dirichlet problem with the boundary conditions

$$u|_\Gamma = p, \quad \Gamma = \partial\Omega, \tag{1.2}$$

a boundary layer is formed near the boundary section Γ_- toward which a flux of particles is transported by the field $\mathbf{b}$. Here, $\Gamma_- = \{\mathbf{x} \in \Gamma : \mathbf{b}(\mathbf{x})\cdot\mathbf{n} > 0\}$ and $\mathbf{n}$ is the outward normal to $\Gamma = \Gamma_+ \cup \Gamma_-$. As $\varepsilon \longrightarrow 0$, the convection term $\mathbf{b}\cdot\nabla u$ becomes dominating but the convective (degenerate) solution u_0 satisfying Eq. (1.1) with $\varepsilon = 0$ and the boundary conditions specified on Γ_+ does not generally satisfy the condition on Γ_-. This condition is fulfilled only if we take into account the diffusion term $-\varepsilon\Delta u$, in which case a boundary-layer solution arises in an $O(\varepsilon)$ neighborhood of Γ_-.

Interior layers in the solution of problem (1.1), (1.2) are formed, for example, along the discontinuity lines (or surfaces for $n = 3$) of u_0, which issue from the points (or lines) $\boldsymbol{\xi}_i \in \Gamma_+$ at which $p(\boldsymbol{\xi})$ ($\boldsymbol{\xi} \in \partial\Omega$) has jump discontinuities. In $u(\mathbf{x})$, these discontinuities are smoothed by diffusion. However, when ε is small, an abrupt change in function values still occurs in their neighborhoods. The mechanism of instability that arises in traditional numerical methods due to boundary and interior layers has been well studied up to this day. Various approaches have been developed to cope with this difficulty. They include both adaptive grid refinement, i.e., a decrease in the local Peclet number $h\mathrm{Pe} = |\mathbf{b}|h/(2\varepsilon)$ (where h is the characteristic size of the grid cell and $\mathrm{Pe} = \max(|\mathbf{b}|/2\varepsilon)$ [3–6], and explicit allowance for the solution's boundary-layer structure by choosing basis functions similar in form to those in [7, 8] or by choosing characteristic directions similar to those in [9]. Meshless methods (in particular, the Petrov–Galerkin local scheme [10]) are becoming highly popular at present. The local Green's function method described here is a version of the Petrov–Galerkin scheme with specially chosen test functions (projectors) that take into account the structure of the solution. The

basic idea of the method has been known for a long time, and it can be illustrated well by the following heuristic considerations.

Let us consider a variational statement of the Dirichlet problem for an operator equation $\mathcal{L}u = f$. The weak solution of the problem is an element $u \in U$ satisfying

$$(\mathcal{L}u, v) = (f, v) \quad \forall v \in V. \tag{1.3}$$

Here, U and V are Hilbert spaces of functions satisfying boundary condition (1.2) for U and the homogeneous condition $v|_\Gamma = 0$ for V.

For Eq. (1.1), the bilinear functional in (1.3) is usually reduced through integration by parts to the form

$$(\mathcal{L}u, v) = \iint_\Omega [\varepsilon \nabla u \cdot \nabla v + (\mathbf{b} \cdot \nabla u)v + cuv] d\Omega, \tag{1.4}$$

and U and V are defined as the closures of spaces of continuous functions with respect to the L_2 norm. Here and below,

$$(u, v) = \iint_\Omega u \cdot v d\Omega.$$

Let $U_N \subset U$ and $V_N \subset V$ be the linear spans of systems of bases functions $\{\varphi_j\}_{j=1}^N$ and $\{\psi_i\}_{i=1}^N$ in U and V, respectively. Then, according to the Petrov–Galerkin scheme, an approximate weak solution of the problem in question is an element

$$u_N = \sum_{j=1}^N c_j \varphi_j \in U_N, \tag{1.5}$$

that satisfies the N variational conditions

$$(\mathcal{L}u_N, \psi_i) = (f, \psi_i), \quad i = 1, 2, \ldots, N. \tag{1.6}$$

These conditions give a linear algebraic system

$$A\mathbf{c} = \mathbf{f} \tag{1.7}$$

for the unknown coefficient vector $\mathbf{c} = (c_1, \ldots, c_N)^T$. The elements $a_{ij} = (\mathcal{L}\varphi_j, \psi_i)$ of the system matrix and the components $f_i = (f, \psi_i)$ of the right-hand-side vector are expressed in terms of the basis functions chosen.

To ensure the norm of residual tending to zero as $N \longrightarrow \infty$, the system of projectors $\{\psi_i\}_{i=1}^N$ must be an ultimate dense set in the Hilbert space under consideration [11].

It is well known that the traditional Galerkin scheme with $\psi_i = \varphi_i$ gives good results for boundary value problems of the elliptic type [12]. However, in the case of a singular perturbation, the boundary layers give rise to spurious oscillations in the approximate solution, which rapidly spread to the entire domain as ε decreases. As a result, the method becomes inapplicable even with modest Peclet numbers.

Numerical stability (i.e., the method's convergence independent of ε) can be achieved through a special choice of the form of ψ_i. Ideally, ψ_i are defined as the local Green's functions of the adjoint problem. Indeed, by using the adjoint operator $\mathcal{L}^* : (\mathcal{L}u, v) = (u, \mathcal{L}^*v)$, variational equality (1.6) can be written as

$$(u_N - u, \mathcal{L}^*\psi_i) = 0. \tag{1.8}$$

Let ψ_i be specified by a shape function ψ defined at the nodes $\mathbf{x}_i$ of a grid covering $\Omega : \psi_i(\mathbf{x}) = \psi(\mathbf{x} - \mathbf{x}_i)$, $i = 1, 2, \ldots, N$. If ψ is a fundamental solution of the adjoint equation

$$\mathcal{L}^*\psi = \delta(\mathbf{x}), \tag{1.9}$$

where $\delta(\mathbf{x})$ is Dirac's delta function, then (1.8) implies that the approximate solution coincides with the exact one at the grid points:

$$u_N(\mathbf{x}_i) = u(\mathbf{x}_i), \quad i = 1, 2, \ldots, N. \tag{1.10}$$

In other words, the use of the Green's functions for the adjoint operator as projectors is equivalent to finding the exact solution of the original problem in a grid norm. As a rule, however, the solution to problem (1.9) cannot be obtained explicitly, for example, for an arbitrary inhomogeneity of the field $\mathbf{b}(\mathbf{x})$. In [13],

the shape function $\psi(\mathbf{x})$ was defined as a fundamental solution of an operator $\hat{\mathcal{L}}$ that approximates $\mathcal{L}^*$ in a small neighborhood Ω_h of zero. Preliminary results have shown that the ε-independent convergence of u_N to u at the nodes $\mathbf{x}_i$ also holds in this case.

2. LOCAL GREEN'S FUNCTIONS

Consider problem (1.9) in $\mathbb{R}^2$: $\mathbf{x} = (x, y)$. For simplicity, let $\mathbf{x}_i$ be the nodes of a rectangular grid covering Ω with a uniform mesh size h, and let the basis functions be conventionally defined as

$$\varphi_j(\mathbf{x}) = \varphi\left(\frac{x - x_j}{h}\right)\varphi\left(\frac{y - y_j}{h}\right), \quad \varphi(t) = \begin{cases} 1 - |t|, & |t| \le 1, \\ 0, & |t| > 1, \end{cases}$$

which ensures a piecewise linear approximation of the exact solution.

According to (1.5), $\mathcal{L}$ is approximated by the sum of the operators $\mathcal{L}_j$ defined on $\Omega_j : |x - x_j| < h, |y - y_j| < h$ and having constant coefficients $\mathbf{b}_j = \mathbf{b}(\mathbf{x}_j)$ and $c_j = c(\mathbf{x}_j)$. For constructing ψ, the following problem naturally arises on the elementary cell $\Omega_h : |x| < h, |y| < h$:

$$\hat{\mathcal{L}}\psi = \delta(\mathbf{x}), \quad \mathbf{x} \in \Omega_h, \quad \psi|_{\Gamma_h} = 0, \quad \Gamma_h = \partial\Omega_h. \tag{2.1}$$

Here, $\hat{\mathcal{L}}\psi \equiv -\varepsilon\Delta\psi - \mathbf{b} \cdot \nabla\psi + c\psi$ is the adjoint differential operator arising in integration by parts in (1.4):

$$(\mathcal{L}u, \psi) = (u, \hat{\mathcal{L}}\psi) + \varepsilon \oint_{\Gamma_h} u \frac{\partial\psi}{\partial n} d\boldsymbol{\xi}, \tag{2.2}$$

$\boldsymbol{\xi}(t) \in \Gamma_h$ is the current point on the boundary of Ω_h, and $t \in [0, 8h]$ is a parameter defining the location of $\boldsymbol{\xi}$ on Γ_h. The coefficients ε, $\mathbf{b}$, and c in $\hat{\mathcal{L}}$ are the constants equal to the values of the corresponding functions at $\mathbf{x}_i$. The index i in (2.1) and (2.2) is omitted for simplicity, but it should be kept in mind that, in the case of variable coefficients, the operators $\hat{\mathcal{L}}$ and, accordingly, the shape functions ψ defined by problem (2.1) are generally different for different ψ_i.

Note that the operator of problem (2.1) is not adjoint even for approximating operators $\mathcal{L}_j$ with constant coefficients, since $(\mathcal{L}u, \psi) \neq (u, \hat{\mathcal{L}}\psi)$ because of the integral over $\partial\Omega_h$ on the right-hand side of (2.2). Thus, even an exact solution of this problem does not give an exact solution at grid points in the sense of (1.9) and (1.10). However, $\hat{\mathcal{L}}$ retains the basic features of an adjoint operator; therefore, we can expect that the solution of problem (2.1) preserves the properties that ensure the numerical stability of the Petrov–Galerkin scheme as $\varepsilon \longrightarrow 0$.

The functions ψ_i defined by solutions to problem (2.1) are called the *local Green's functions* of the adjoint equation, unlike the *global Green's function* (or a fundamental solution) $g(\mathbf{x})$ satisfying $\hat{\mathcal{L}}g = \delta(\mathbf{x})$ in the whole space $\mathbb{R}^d$. For the two-dimensional problem ($d = 2$), the functions $g(\mathbf{x})$ can be written explicitly in terms of the modified Bessel function K_0, which has an expected logarithmic singularity at $\mathbf{x} \longrightarrow 0$.

In [13], ψ was represented in terms of g and a contour integral of the unknown normal derivative $\partial\psi/\partial n$ on the boundary:

$$\psi(\mathbf{x}) = g(\mathbf{x}) + \oint_0^{8h} g(\mathbf{x} - \boldsymbol{\xi}(t))\nu(t)dt. \tag{2.3}$$

Here, $\nu(t) = \varepsilon\partial\psi(\boldsymbol{\xi})/\partial n|_{\boldsymbol{\xi} = \boldsymbol{\xi}(t)}$. Next, $\nu(t)$ was determined from an integral equation arising when the condition $\psi|_{\Gamma_h} = 0$ is satisfied.

Replacing ν in (1.6) by a function ψ_i of form (2.3) defined at $\mathbf{x}_i$ gives the elements a_{ij} ($j = 1, 2, \ldots, N$) of the ith row in the matrix of system (1.7). They are expressed in terms of the third-order matrix stencils $B =$

$[b(p_1, p_2)]$ ($p_1, p_2 = -1, 0, 1$) according to the rule

$$a_{ij} = b(p_1, p_2), \quad p_1 = (x_i - x_j)/h, \quad p_2 = (y_i - y_j)/h.$$

Using the notation of [13], we have

$$B = \begin{pmatrix} I^+_{-1} + J^+_{-1} & I^+_0 & I^+_1 - J^-_{-1} \\ J^+_0 & 1 & -J^-_0 \\ -I^-_{-1} + J^+_1 & -I^-_0 & -I^-_1 - J^-_1 \end{pmatrix}, \tag{2.4}$$

$$I^\pm_{p_2} = \int_{-h}^{h} v^\pm_x(y)\varphi(y/h + p_2)dy, \quad J^\pm_{p_1} = \int_{-h}^{h} v^\pm_y(x)\varphi(x/h + p_1)dx, \tag{2.5}$$

where $v^\pm_x = \varepsilon\partial u/\partial x|_{x = \pm h}$ and $v^\pm_y = \varepsilon\partial u/\partial y|_{y = \pm h}$ are the values of the unknown function $\pm v(t)$ on the corresponding sides of the square cell Ω_h (in the local coordinates x and y with the origin at the node $\mathbf{x}_i$). Note that, when $|x_i - x_j| \geq 2h$ or $|y_i - y_j| \geq 2h$, the supports of ψ_i and φ_j do not intersect; i.e., $I^\pm_{p_2}, J^\pm_{p_1} \equiv 0$. Consequently, $a_{ij} = 0$ for i and j such that $|p_1| \geq 2$ or $|p_2| \geq 2$.

Thus, when we use (2.3), the stencil B of the matrix A of system (1.7) can be expressed in terms of integrals of $v(t)$. As a result, the function $\psi(\mathbf{x})$ itself does not actually need to be constructed. The analysis performed in [13] showed that the stencil thus constructed gives a matrix A that possesses the properties of M matrix [15], which ensure that the Gauss–Seidel solution of system (1.7) converges rapidly. Moreover, the elements of the stencil stabilize as $\varepsilon \longrightarrow 0$. As a result, the node convergence

$$u_N(\mathbf{x}_i) \longrightarrow u(\mathbf{x}_i) \text{ as } N \longrightarrow \infty$$

holds in the presence of the boundary and interior layers.

However, for high values of the local Peclet number, starting with h Pe $\approx 10^5 \div 10^7$, the computational costs associated with finding $v(t)$ and constructing the matrix of system (1.7) were found to increase abruptly, although the method kept exhibiting stable convergence. This limitation of the method can be overcome by using an asymptotic representation of $\psi(\mathbf{x})$ as $\varepsilon \longrightarrow 0$ (Pe $\longrightarrow \infty$).

3. ASYMPTOTICS OF LOCAL GREEN'S FUNCTIONS

In addition to (2.3), an explicit representation of the solution of problem (2.1) can be derived (by separation of variables) in the form of a double series in the eigenfunctions $\hat{u}_{mn} : \hat{\mathcal{L}}\hat{u}_{mn} = \lambda_{mn}\hat{u}_{mn}$ of the differential operator $\hat{\mathcal{L}}$ on Ω_h:

$$\psi(x, y) = \sum_{m=0}^{\infty}\sum_{n=0}^{\infty} f_{mn}\hat{u}_{mn}(x, y)/\lambda_{mn}. \tag{3.1}$$

In the case under consideration,

$$\lambda_{mn} = [d + \varepsilon_h^2(m^2 + n^2)]/(4\varepsilon), \quad d = b^2 + 4\varepsilon c, \quad b^2 = |\mathbf{b}|^2, \quad \varepsilon_h = \pi\varepsilon/h,$$
$$\hat{u}_{mn}(x, y) = \hat{u}_{1,m}(x)\hat{u}_{2,n}(y), \quad \hat{u}_{i,k}(\xi) = \exp[-b_i\xi/(2\varepsilon)]s_k(\xi), \tag{3.2}$$
$$s_k(\xi) = \sin[(\xi + h)\pi k/(2h)], \quad i = 1, 2, \quad k = m \text{ or } n.$$

The eigenfunctions u_{mn} of the original operator $\mathcal{L}$ are obtained from (3.2) by replacing $-b_i$ with b_i in the exponentials with the eigenvalues λ_{mn} remaining the same. Since the eigenfunctions u_{mn} and $\hat{u}_{mn}$ are biorthogonal, i.e.,

$$(u_{mn}, \hat{u}_{kl}) = 0 \text{ for } m \neq k \text{ or } n \neq l,$$

the expansion coefficients f_{mn} can easily be derived in the explicit form:

$$f_{mn} = (\delta, u_{mn})/(u_{mn}, \hat{u}_{mn}) = u_{mn}(0, 0)/h^2.$$

It should be noted that, although (3.1) is given in a closed analytical form, its direct use in the computations is not profitable, since the convergence of the series is ensured only by the quadratic growth of the eigenvalues involved in the denominator: $\lambda_{mn} \sim O(m^2 + n^2)$ as $m^2 + n^2 \longrightarrow \infty$; however, for $\varepsilon/h \ll 1$, the coefficient ε_h of $(m^2 + n^2)$ sharply reduces this growth. The computational costs become even greater when we sum the series for $v(t)$, whose convergence is one order of magnitude slower.

On the other hand, series (3.1) can be transformed into a form convenient for deriving asymptotics. First, it is obvious that $f_{mn} \equiv 0$ for even indices. Next, for $v_x^{\pm}(y)$ and $v_y^{\pm}(x)$ involved in the stencil, the double series is reduced to a singlefold one if we use formula 5.1.26.7 from [16]:

$$\sum_{m=0}^{\infty} \frac{(-1)^m(2m+1)}{a^2 + (2m+1)^2} = \frac{\pi}{4\mathrm{ch}(h\pi a/2)}.$$

As a result,

$$v_x^{\pm} = \mp\frac{1}{h} e^{-[b_1(\pm h) + b_2 y]/(2\varepsilon)} R(y), \quad v_y^{\pm} = \mp\frac{1}{h} e^{-[b_1 x + b_2(\pm h)]/(2\varepsilon)} R(x),$$
$$R(\xi) = \sum_{k=0}^{\infty} (-1)^k s_{2k+1}(\xi) e^{-ha_k/(2\varepsilon)}/(1 + e^{-ha_k/\varepsilon}), \quad a_k^2 = d + \varepsilon_h^2(2k+1)^2, \tag{3.3}$$

where s_k is given in (3.2).

The series $R(\xi)$ still converges slowly for $\varepsilon/h \ll 1$. To construct its asymptotics as $\varepsilon \longrightarrow 0$, we use the Poisson formula [17]:

$$\sum_{n=-\infty}^{\infty} f(n) = \sum_{n=-\infty}^{\infty} \int_{-\infty}^{\infty} f(x) e^{2i\pi n x} dx,$$

which yields the representation

$$R(\xi) = \frac{1}{2} \sum_{n=-\infty}^{\infty} A_n(\xi), \tag{3.4}$$

where

$$A_n(\xi) = (-1)^{n+1}\lambda(I_n^+ - I_n^-)/4, \quad \lambda = h/\varepsilon,$$
$$I_n^{\pm}(\xi) = \int_{-\infty}^{\infty} f(t)\exp[-\lambda S_n^{\pm}(\xi, t)]dt, \quad f(t) = \left(1 + e^{-\lambda\sqrt{d + (\pi t)^2}}\right)^{-1},$$
$$S_n^{\pm}(\xi, t) = -it(\pi/2 + \pi n \pm z) + \sqrt{d + (\pi t)^2}/2,$$
$$z = (\xi + h)\pi/(2h), \quad \xi \in [-h, h], \quad z \in [0, 1].$$

Each of the functions $S_n^{\pm}$ has a single saddle point of minimum height $t_n^{\pm}$:

$$t_n^{\pm} = i\sqrt{d/(2p_n^{\pm})}(2n + 1 \pm 2z/\pi),$$
$$p_n^{\pm} = 2z^2 \pm 2\pi(2n+1)z + \pi^2(2n^2 + 2n + 1).$$

According to the steepest descent method, their contribution to the asymptotics of $I_n^{\pm}$ is given by

$$I_n^{\pm} = \sqrt{2\pi/(\lambda S_{n,2}^{\pm})} f(t_n^{\pm}) \exp(-\lambda S_{n,0}^{\pm})[1 + O(1/\sqrt{\lambda})], \quad \lambda \longrightarrow \infty.$$

Here, $S^{\pm}_{n,0} = S^{\pm}_n(\xi, t^{\pm}_n) = \sqrt{dp^{\pm}_n/(2\pi^2)}$ and $S^{\pm}_{n,2} = \partial^2 S^{\pm}_n/\partial t^2\big|_{t=t^{\pm}_n} = \sqrt{2p^{\pm}_n/(d\pi^2)}\,p^{\pm}_n$.

A comparative analysis of the functions $S^{\pm}_{n,0}(\xi)$, which determine the order of the exponential decay, shows that, for $\xi \in [-h, h]$, a major contribution to $R(\xi)$ is made by four terms of the series with $n = -2, -1, 0, 1$. Compared with them, the contribution made by the other terms is exponentially small. Thus, as $\varepsilon \longrightarrow 0$, we do not need to solve integral equations or sum series in order to determine $v(t)$, while the integration of explicit asymptotic representations in (2.5) does not require considerable computational costs.

As an illustration, the table presents the numerical results for the example considered in [13] for the square domain $0 \le x, y \le 1$ with the right-hand side f corresponding to the exact solution

$$u(x, y) = x^2y^2[1 - e_1(x)][1 - e_2(y)], \quad e_n(x_n) = \exp[-(1 - x_n)/\varepsilon], \quad n = 1, 2,$$

and with boundary layers developing near the outlet edges $x = 1$ and $y = 1$; $\mathbf{b} = (b\cos\theta, b\sin\theta)$, $\theta = \pi/8$, $c = 1$, the mesh size is $h = 0.01$, and $N = 100 \times 100 = 10^4$. For various ε, the table lists the average error

$$r_h = N^{-1}\sum_{i=1}^{N}|u(\mathbf{x}_i) - c_i| \approx \iint_{\Omega}|u - u_N|\,d\Omega$$

and the total computation time (in seconds) taken on a 733 MHz computer. The columns denoted by I list the results of [13] obtained by solving integral equations to determine v; the columns denoted by II correspond to v defined by series (3.3) (for $\varepsilon = 10^{-3}$) or by asymptotics (3.4) (for $\varepsilon \le 10^{-5}$). In both cases, $f(x, y)$ is approximated on a given grid by a piecewise constant function, which introduces an additional error. For this reason, columns III list the results obtained also by using (3.3) and (3.4), but through calculating the components $f_i(f, \psi_i)$ of the right-hand side by numerical integration instead of the piecewise approximation. The table shows that the use of asymptotics considerably reduces the computational costs while the accuracy remains the same. When f_i is found through integration, the accuracy improves by one order of magnitude but the computational costs again increase. In this case, however, they also do not increase sharply and stabilize as $\varepsilon \longrightarrow 0$ as in the case of the error.

It should be noted that most of the computational time is required for constructing the matrix (stencil) and the right-hand side of system (1.7), while its solution itself usually requires only a few iterations of the Gauss–Seidel method (in the example considered above, $N_{it} = 9$ in case I and $N_{it} = 2$ in cases II and III for $\varepsilon \le 10^{-5}$).

4. INTERIOR LAYERS, CURVED BOUNDARIES, AND INHOMOGENEOUS FIELDS

In the example considered above, when ε is small, no nodes are located within the boundary layers. For this reason, it may seem that the method proposed produces only a degenerate solution u_0 not satisfying all the boundary conditions. Examples of solutions to problems with interior layers show that this is not the case: the method yields a nodal approximation to the full solution $u(\mathbf{x})$ with steep gradients in layers.

For example, Fig. 1 shows the solution of the problem for homogenous equation (1.1) (with $f \equiv 0$) and discontinuous boundary conditions (1.2): $p = 1$ on a part of the boundary Γ_+ ($x = 0$, $0.25 \le y \le 0.5$), and $p = 0$ on the remaining Γ; $\varepsilon = 10^{-7}$, $b = c = 1$, $\theta = \pi/8$, $h = 0.02$, $N = 2500$, and $t = 1$ s.

In the solution of this problem, two interior layers are formed extending from the discontinuity points of the boundary conditions along the lines defined by the convective flux $\mathbf{b}$ and a boundary layer is formed on

Table

ε	Columns					
	I		II		III	
	r_h	t	r_h	t	r_h	t
10^{-3}	0.0021	2	0.0021	2	0.00047	132
10^{-5}	0.0030	7	0.0030	<1	0.00018	58
10^{-7}	0.0025	43	0.0025	<1	0.00020	56
10^{-9}	0.0025	116	0.0025	<1	0.00020	54

the right boundary $x = 1, 0 \le y \le 1$. As should be expected, away from discontinuity points, the interior layers are gradually smoothed due to diffusion. Despite the sharp change in $u(\mathbf{x}_i)$ at the nodes lying on the different sides of the layers, the numerical solution is stable for any $\varepsilon \ll 1$.

The low computational costs required by the method also make it possible to rapidly obtain results for equations with variable coefficients, when the functions ψ_i have to be generally constructed for each of the N nodes $\mathbf{x}_i$. As an example, Fig. 2 shows the field $\mathbf{b}(\mathbf{x}) = (1.5\sin\varphi, -0.5\cos\varphi)$, where φ is the polar angle of the point (x, y) in coordinates with the origin at $\mathbf{x}_0 = (0, 0.5)$, and the plot of the corresponding solution u_N obtained with $f \equiv 0$ and $p \ne 0$ only on the interval $x = 0, 0.8 \le y \le 1$, $\varepsilon = 10^{-9}$, $c = 1$, $N = 2500$, $N_{it} = 85$, and $t = 118$ s.

In the examples considered, Ω is exactly partitioned into subdomains Ω_i by a square grid. For domains with curved boundaries, the use of bases φ_i and ψ_j with square or rectangular elementary cells actually means that Ω is approximated by a domain with a steplike boundary. However, the nodal convergence of the numerical solution u_N to the exact solution u as $h \longrightarrow 0$ is also retained in this case. As an illustration, we consider Hemker's example [18] for a domain with a circular hole $\Omega_c : x^2 + y^2 \le 1$ and with the horizontal convective flux $b = (1, 0)$. Equation (1.1) is homogeneous ($f \equiv 0$), and the Dirichlet conditions $u|_{\Gamma_c} = 1$ are set on the hole's boundary $\Gamma_c = \partial\Omega_c$.

For the whole space with the circle $\Omega = \mathbb{R}^2 \backslash \Omega_c$ cut out, the solution $u(x, y)$ is exactly constructed in the form of a series in cylinder functions. This solution describes the transport of particles from the source (the boundary Γ_c) along the semiinfinite strip $|y| < 1, x > \sqrt{1 - y^2}$ with interior layers formed at the strip's boundary $y = \pm 1$, $x > 0$. In the numerical solution, the space $\mathbb{R}^2$ was restricted by the rectangle $-3 \le x \le 13$, $|y| < 6$ with the homogeneous Dirichlet conditions $u = 0$ set on the left and horizontal sides and with the Neumann condition $u'_x|_{\Gamma_+} = 0$ set on the right boundary $\Gamma_+ : x = 13$, $|y| < 6$. The latter condition prevented the formation of a boundary layer, which is absent in the exact solution.

Figure 3 shows the plot of $u_N(x, y)$ obtained for the same parameters as in [18] ($\varepsilon = 0.2$, $c = 0$) with the mesh size $h = 0.2$. Although Γ_c is approximated quite roughly for this h, the resulting solution agrees well with the exact one. This can be seen when the numerical solution is compared with the exact solution along the cross sections at $x = 1.4$ and $x = 11$, $|y| < 6$, i.e., near the source and far from it (Fig. 4).

Since the series describing the exact solution converge poorly for small ε, the comparison shown in Fig. 4 corresponds to $\varepsilon = 0.04$. The stars indicate the values obtained for $h = 0.2$ ($N = 4872$, $N_{it} = 46$, $t = 4$ s) and the circles correspond to $h = 0.1$ ($N = 19204$, $N_{it} = 136$, $t = 10$ s). It can be seen that, even in the zone of layers, the values of $u_N(\mathbf{x}_i)$ steadily approach the exact solution as h decreases, despite the steplike approximation of Γ_c.

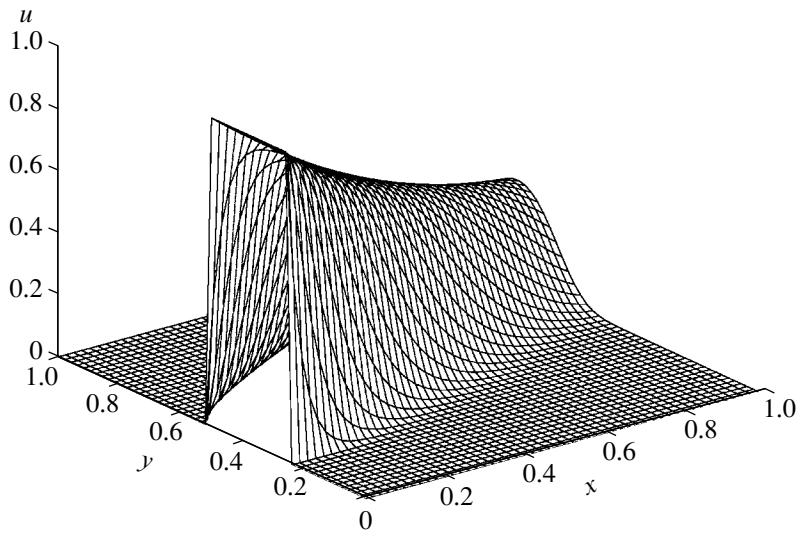

Fig. 1.

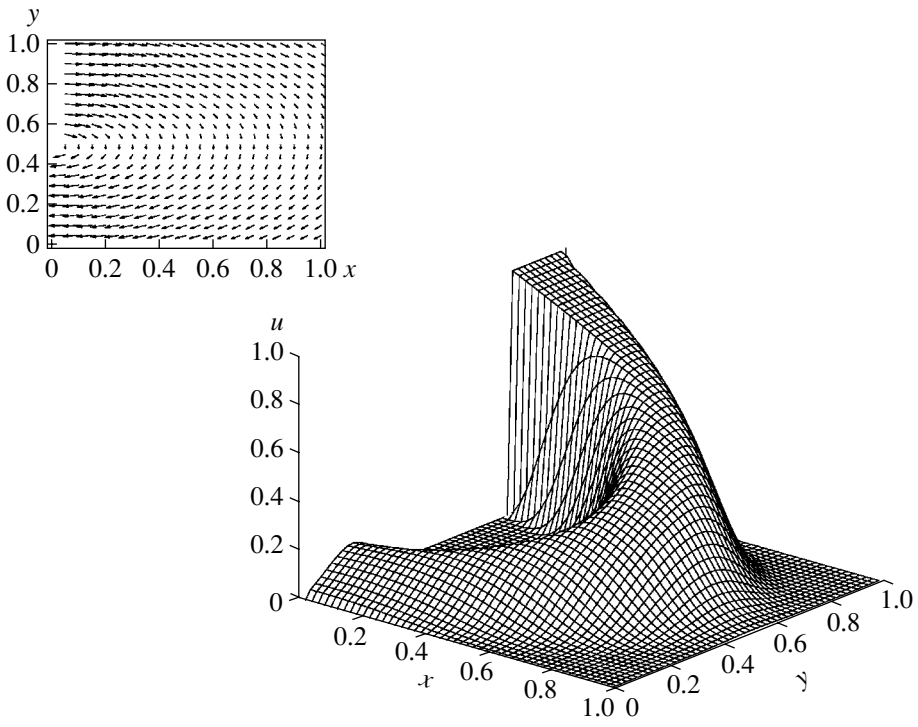

Fig. 2.

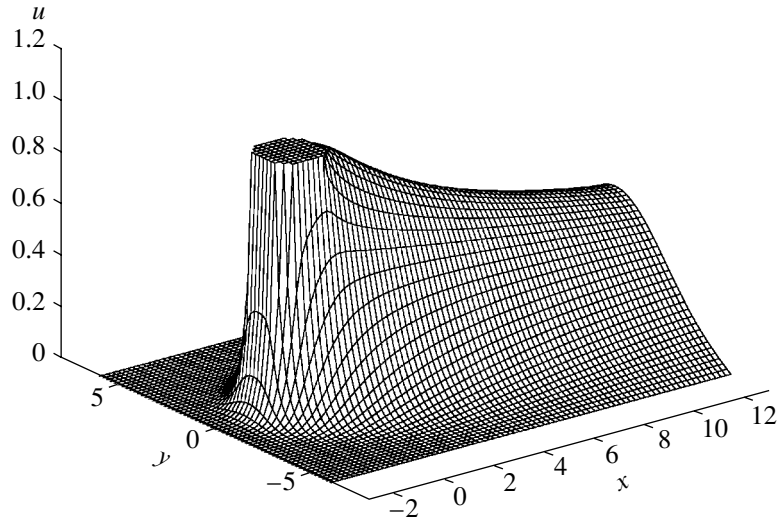

Fig. 3.

Remark. When constructing ψ_i, we can use as Ω_h not only $2h \times 2h$ squares but also differently shaped cells, for example, circles $x^2 + y^2 \le h^2$. In this case, the form of the matrix stencil B changes and even the straight line segments of Γ become approximated. However, as in the example considered above, this circumstance does not degrade the general convergence as $h \longrightarrow 0$. At the same time, the use of circular cells reduces the computational costs, because, for a variable field $\mathbf{b} = (b\cos\theta, b\sin\theta)$ and $c = \text{const}$, the functions ψ_i actually depend only on b and, for different θ, they are transformed into each other by rotations through suitable angles.

The mechanism of convergence can be better understood by taking into account the following property of the normal derivative $\partial\psi/\partial n$ on the boundary of Ω_h.

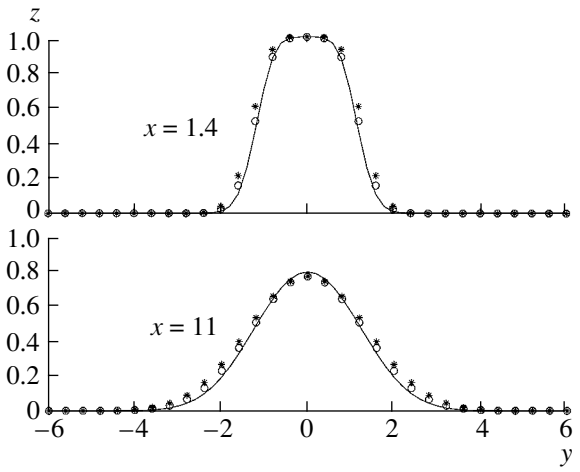

Fig. 4.

Lemma. *Let t_0 be the coordinate of the point $\boldsymbol{\xi}_0 = \boldsymbol{\xi}(t_0) \in \Gamma_h$ at which the field line of* **b** *passing through the center of Ω_h intersects the boundary. The function $v(t) = \varepsilon\partial\psi/\partial n$ is maximal at this point and decays exponentially outside its vicinity as $\varepsilon/h \longrightarrow 0$ so that $v(t)$ converges to $-q\delta(t - t_0)$, where $q = \exp[-ch/\max(|b_1|, |b_2|)]$ is independent of ε and δ is Dirac's delta function.*

The proof follows from a direct calculation of the limit of the integral $\int_0^{8h} f(t)v(t)dt$ with an arbitrary continuous function $f(t)$ using the representations and asymptotics derived for $v(t)$.

Returning to (1.8)–(1.10), we obtain, instead of (1.10), the condition

$$u_N(\mathbf{x}_i) - qu_N(\boldsymbol{\xi}_i) \sim u(\mathbf{x}_i) - qu(\boldsymbol{\xi}_i)$$

as $\varepsilon/h \longrightarrow 0$, which does not contradict the nodal convergence $u_N(\mathbf{x}_i) \longrightarrow u(\mathbf{x}_i)$ when $c > 0$ and $q < 1$. The latter condition is also a necessary condition for stencil (2.4) to give an M matrix in which the row sum of the absolute values of all the off-diagonal elements must be less than the diagonal unit.

5. CONCLUSION

A two-dimensional boundary value problem for the convection–diffusion equation was used to demonstrate the high efficiency of the local Green's function method as applied to singularly perturbed problems. A grid discretization based on local Green's functions yields a system of algebraic equations with a sparse M matrix, which can be solved by iterative methods. The convergence rate of the iterative solution becomes even higher when ε decreases; i.e., the method is more efficient when the singular perturbation is more severe. In our view, no fundamental difficulty should arise in implementing the method in the case of three variables.

ACKNOWLEDGMENTS

We are grateful to Professor O. Axelsson (the Netherlands), who indicated the advantages of the underlying method and, thus, initiated our research in this field within the joint NWO-RFBR, project no. 047-008-007. This work was also supported by the Russian Foundation for Basic Research, project no. 03-01-96626.

REFERENCES

1. M. I. Vishik and L. A. Lyusternik, "Regular Degeneration and Boundary Layer for Linear Differential Equations with a Small Parameter," Usp. Mat. Nauk **12** (5), 3–122 (1957).
2. A. B. Vasil'eva and V. F. Butuzov, *Asymptotic Expansions of Solutions of Singularly Perturbed Equations* (Nauka, Moscow, 1973) [in Russian].
3. N. S. Bakhvalov, "Optimization of Methods for Boundary Value Problems Involving a Boundary Layer," Zh. Vychisl. Mat. Mat. Fiz. **9**, 841–859 (1969).

4. E. P. Doolan, J. J. H. Miller, and W. H. A. Schilders, *Uniform Numerical Methods for Problems with Initial and Boundary Layers* (Boole, Dublin, 1980; Mir, Moscow, 1983).
5. G. I. Shishkin, *Grid Approximations of Singularly Perturbed Elliptic and Parabolic Equations* (Ural. Otd., Ross. Akad. Nauk, Yekaterinburg, 1992) [in Russian].
6. H. Roos, M. Stynes, and L. Tobiska, *Numerical Methods for Singularly Perturbed Differential Equations* (Springer-Verlag, Heidelberg, 1996).
7. P. W. Hemker, PhD Thesis (Math. Center, Amsterdam, 1977).
8. O. Axelsson, "Stability and Error Estimates of Galerkin Finite Element Approximations for Convection–Diffusion Equations," IMA J. Numer. Anal., No. 1, 329–345 (1981).
9. L. S. Xanthis and C. Schwab, "The Method of Arbitrary Lines," C. R. Acad. Sci., Ser. I **312**, 181–187 (1991).
10. S. N. Atluri and S. Shen, "The Meshless Local Petrov–Galerkin (MLPG) Method: A Simple and Less-Costly Alternative to the Finite Element and Boundary Element Methods," Comput. Model. Eng. Sci. **3** (1), 11–51 (2002).
11. M. A. Krasnosel'skii, G. M. Vainikko, P. P. Zabreiko, *et al.*, *Approximate Solution of Operator Equations* (Nauka, Moscow, 1969) [in Russian].
12. G. I. Marchuk and V. I. Agoshkov, *Introduction to Projection Grid Methods* (Nauka, Moscow, 1981) [in Russian].
13. O. Axellson, E. V. Glushkov, and N. V. Glushkova, "The Local Green's Function Method for Singularly Perturbed Convection–Diffusion Problems," Dokl. Akad. Nauk **388**, 166–170 (2003) [Dokl. Math. **67**, 98–102 (2003)].
14. K. W. Morton, *Numerical Solution of Convection–Diffusion Problems* (Chapman & Hall, London, 1996).
15. Yu. A. Kuznetsov and V. V. Voevodin, *Matrices and Computations* (Nauka, Moscow, 1984) [in Russian].
16. A. P. Prudnikov, Yu. A. Brychkov, and O. I. Marichev, *Integrals and Series: Elementary Functions* (Nauka, Moscow, 1981) [in Russian].
17. M. V. Fedoryuk, *Asymptotics: Integrals and Series* (Nauka, Moscow, 1987) [in Russian].
18. P. W. Hemker, "A Singularly Perturbed Model Problem for Numerical Computation," J. Comput. Appl. Math, No. 76, 237–285 (1996).